

Evolution of the transport critical current density and irreversibility field as a function of heat treatment and pressing pressure during processing of Ag-sheathed (Bi,Pb)₂Sr₂Ca₂Cu₃O_x tapes

H. S. Edelman,^{a),b)} J. A. Parrell,^{c)} and D. C. Larbalestier^{a),c)}
Applied Superconductivity Center, University of Wisconsin, Madison, Wisconsin 53706

(Received 12 September 1996; accepted for publication 18 November 1996)

Extended electric field-current density characteristics taken on the bare cores of monofilament (Bi,Pb)₂Sr₂Ca₂Cu₃O_x (2223) tapes at 77 K have been used to measure the irreversibility field, H^* , and the critical current density, J_c , at different stages of tape processing. The number of heat treatments and the uniaxial pressing pressure were the experimental variables. Both H^* and J_c increased substantially with heat treatment and with deformation pressure. The data are consistent with an improvement in J_c from two factors, one being an increase in the 2223 phase fraction with increasing heat treatment, the second, independent cause being an increase in the flux pinning properties of the composite. The experiments show that improving J_c involves control of at least three factors: enhancing the volume fraction of 2223 phase; increasing flux pinning; and enhancement of the connectivity of the grain boundaries that lie within the current path. © 1997 American Institute of Physics. [S0021-8979(97)00705-6]

I. INTRODUCTION

A prerequisite for consistently achieving high critical current density J_c in Ag-sheathed polycrystalline (Bi,Pb)₂Sr₂Ca₂Cu₃O_x (BSCCO) (2223) tapes is an understanding of what limits J_c in particular samples. Conversion of mixed phase precursor powder to the final 2223 phase involves two or more heat treatments with precise control of starting phase assemblage, temperature, oxygen partial pressure, heating and cooling conditions, and the details of the intermediate deformation steps. The very large number of variables in this process makes it difficult to isolate the effects of any one parameter or to understand their interactions. This difficulty is illustrated by a general inability to consistently reproduce the highest J_c from one sample to the next. The goal of virtually all optimizations is to maximize J_c , where J_c is defined by the transport critical current I_c (usually defined at an electric field $E=1 \mu\text{V}/\text{cm}$, $H=0$, and $T=77 \text{ K}$), normalized by the *total* cross-section of the BSCCO core. Important current-limiting factors that depend on processing parameters include cracks,¹ the misalignment of adjacent grains,² intergrowths of the (Bi,Pb)₂Sr₂CaCu₂O_x (2212) phase within the 2223 phase,³ and weak intragranular flux pinning.^{4,5} As with the processing parameters, the central difficulty in sorting out the significance of these different current-limiting factors is their tendency to act simultaneously. Further obscuring the underlying physics of the current-limiting mechanisms is the imprecision of the operational definition of J_c when it is defined, as is usual, to be I_c/A . Variations in J_c defined in this way cannot be easily interpreted if the properties vary *within* a cross-section A , and/or if different current-limiting mechanisms dominate at different stages in the processing. Transport measurements

on different regions of a tape core provide direct evidence for just such transverse inhomogeneity in optimized samples,⁶ and magneto-optical (MO) images⁷⁻⁹ reveal the resulting percolative current flow. Thus, there is an inherent uncertainty involved in optimizing $J_c=I_c/A$ through a process which influences both the intrinsic flux pinning capability of the material *and* the connectivity of the polycrystalline cross-section.

This paper describes an experiment designed to follow some of the above variables throughout the whole heat treatment/fabrication process of a 2223 tape, in order to facilitate identification of the primary current limiting effects. The experiment revealed a strong correlation between J_c ($1 \mu\text{V}/\text{cm}$, $H=0$) and the irreversibility field H^* at 77 K. As earlier noted,⁵ the existence of a well defined H^* can be interpreted as a sign that flux pinning within the grains is controlling the critical current density and that grain boundaries are not controlling the properties. However, we believe that such data are also consistent with J_c being determined at grain boundaries within the current path. We deduce this by comparing the $E(J)$ characteristics of the tapes to those recently measured across the grain boundaries of 2212 bicrystals.^{10,11} Taking account of the fact that the microstructure evolves from one containing substantial 2212 and insulating second phases early in the process, to a largely 2223 phase structure late in the process, we propose that the principal dissipation in optimized tapes at low electric fields is also associated with vortex motion at grain boundaries, and not just within the grains. Such a view is consistent with the "railway switch" model of intergrain transport across strongly coupled, low angle grain boundaries as proposed by Hensel *et al.*² and corroborated by Cho *et al.*¹² The precise relation between the local critical current density determined by flux motion within grains or at grain boundaries and the macroscopic average is still not clear. However, it is noteworthy that $J_c=I_c/A$ for epitaxial 2223 films without grain boundaries ($>10^6 \text{ A}/\text{cm}^2$ at 77 K, 0 T) can be up to two

^{a)}Department of Physics.

^{b)}Now at Seagate Technology, 7801 Computer Avenue South, Minneapolis, MN 55435.

^{c)}Materials Science Program.

orders of magnitude higher than for the best polycrystalline tapes,¹³⁻¹⁵ even though the irreversibility temperatures of the films and tapes are rather similar.¹⁵ Thus, lack of connectivity in polycrystals, whether produced by misaligned grains, lower T_c phase intergrowths, insulating phases, or cracks, is still a very important current-limiting mechanism in tapes, whatever the flux pinning capability of individual grains. In attempting to distinguish the role of all of these various mechanisms, we believe that measurement of H^* seems to be the best diagnostic for distinguishing the flux pinning component from the connectivity component in BSCCO tapes.

II. EXPERIMENT

The tapes were made from a “two-powder” mixture¹⁶ having an overall composition of $\text{Bi}_{1.8}\text{Pb}_{0.4}\text{Sr}_2\text{Ca}_2\text{Cu}_3\text{O}_x$, using an oxide-powder-in-tube fabrication method.¹ Conversion of the precursor powder components [$(\text{Bi,Pb})_{2.2}\text{Sr}_2\text{CaCu}_2\text{O}_y$, CaCuO_2 , and CuO] to nearly phase-pure $(\text{Bi,Pb})_2\text{Sr}_2\text{Ca}_2\text{Cu}_3\text{O}_x$ took place during first and second heat treatments of 50 h each, and a third heat treatment of 100 h, all at 825 °C in 7.5% O_2 /balance N_2 . Between heat treatments, the samples were uniaxially pressed between polished tungsten carbide platens at a pressure of either 0.5 or 2.0 GPa. Thus, the two processing variables studied here were the number of heat treatments and the deformation pressure.

Our principal evaluation technique was the measurement of voltage versus transport current (V vs I) from ~ 3 nV to 1 mV using a Keithley 1801 preamplifier. The nominal electric field $E = V/L$, where $L \approx 6$ mm is the distance between the voltage taps placed on the 2 cm long samples, varied from 0.005 to 1500 $\mu\text{V}/\text{cm}$, and J_c ($1 \mu\text{V}/\text{cm}$, 0 T, 77 K) $= I_c/A$ ranged from 3.8 to 14.5 kA/cm^2 . The cross-sectional area A is the average of measurements by digital image analysis on three to five transverse tape cross-sections. The samples were measured in magnetic fields from 0–500 mT within the liquid N_2 filled bore of a Cu solenoid. The ~ 220 K temperature drop across the voltage circuit generated a thermoelectric voltage via the Seebeck effect. Variations in this baseline were kept to ± 3 nV by using uninterrupted oxygen-free, high-conductivity (OFHC) Cu wires for both voltage leads between the sample and preamplifier.

Each tape was measured after its Ag sheath had been chemically removed in a mixture of two parts 30% H_2O_2 and five parts NH_4OH . A special fixture held the fragile core in a nominally unstressed state. The sample lay across a U-shaped block as shown in Fig. 1, so that it was supported at both ends but surrounded by liquid N_2 in between. One end of the sample was glued to the block, and a shallow U-shaped bracket was fitted over the other end. This bracket prevented the sample from transverse flexing, while allowing the free end of the sample to slide towards or away from the glued end as the sample and block contracted or expanded with changes in temperature.

The microstructures of polished longitudinal cross-sections were examined using a scanning electron microscope (SEM) operated at 15 kV. The phase balance of some samples were analyzed by x-ray diffraction (XRD).

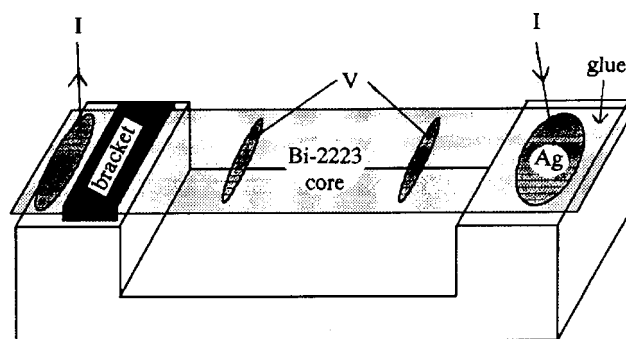


FIG. 1. This figure illustrates how a section of brittle tape core is held to prevent thermal stresses during cooling and warming. The core lies on a U-shaped block, with one end glued to the block and the other end free, allowing the sample to expand or contract with changes in temperature. A bracket over the free end prevents that end from lifting off the block or moving side to side. When the fixture is immersed in liquid N_2 , liquid enters the channel through the center of the block and cools both top and bottom surfaces of the sample.

III. RESULTS

Figure 2 presents SEM photomicrographs, taken in electron backscatter mode, of longitudinal sections of samples at three different stages of processing. Figure 2(a) shows the tape with just one heat treatment. Its dark gray, long, thin 2223 grains are well separated within the still predominately 2212 light gray matrix. Black alkaline earth cuprate (AEC) particles $\sim 5 \mu\text{m}$ long are also visible. It is easy to see that any current path which connects the patchwork of 2223 grains must be percolative and cannot encompass the entire tape volume (or completely fill any given cross-section A). Moreover, it appears that current passage through 2212 grains would be required in some parts of the core. This tape had the lowest J_c ($1 \mu\text{V}/\text{cm}$, 0 T, 77 K), 3.8 kA/cm^2 . Figure 2(b) shows the tape that was pressed at 0.5 GPa between its first two heat treatments. In contrast to the first heat treatment sample, dark gray 2223 now fills most of its core, consistent with the weak 2212 signal observed by XRD. However, even though the fraction of 2212 phase is small, it appears that it may still exist around the 2223 grains, since there is evidence for a light phase outlining many of the 2223 grains. J_c of the sample increased to 9.6 kA/cm^2 . Figure 2(c) shows the tape that was pressed at 2 GPa after each of the first two of its three heat treatments. Essentially no 2212 phase was detectable by either SEM or XRD analysis. The 2223 phase largely fills the core, although some residual AEC particles are still present. This tape had the highest J_c , 14.5 kA/cm^2 .

Figure 3 shows typical $E(J)$ characteristics of the three heat treatments, 2 GPa tape both before and after its Ag sheath had been removed. Current sharing with the Ag causes the curve to bend toward an ohmic characteristic above $\sim 1 \mu\text{V}/\text{cm}$, so that it diverges from the curve for the bare sample. Flux flow in the 2223 core tends to produce a similar characteristic for the bare superconductor above $\sim 100 \mu\text{V}/\text{cm}$. All the tapes were measured first with and then without Ag, and all their $E(J)$ characteristics showed the same behavior at large E . In order to eliminate the effect

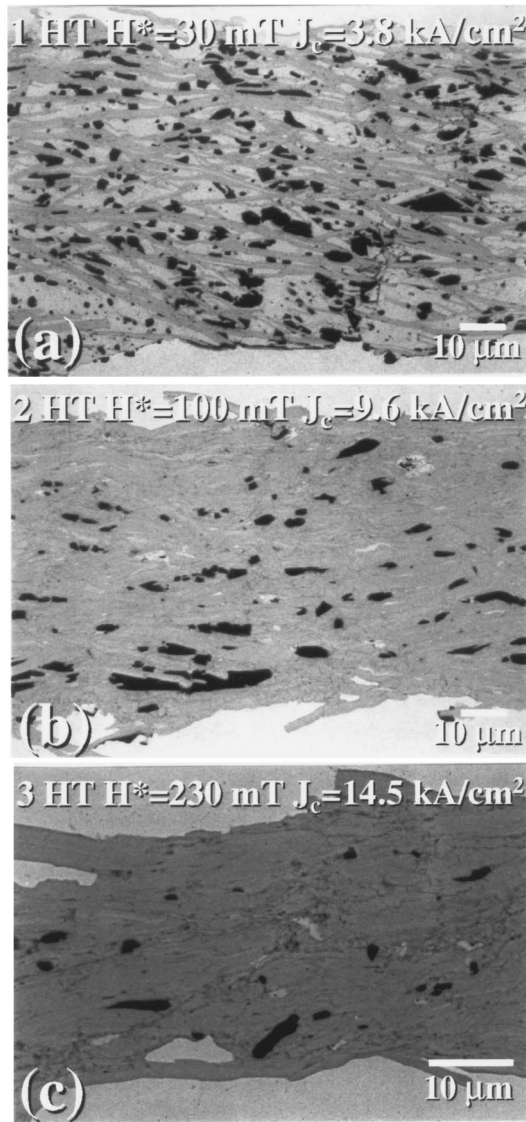


FIG. 2. Scanning electron microscope images of representative tapes in longitudinal section exhibit a microstructural evolution that parallels the evolution of H^* and J_c . Tape (a) had one heat treatment; $H^* = 30 \pm 20$ mT and $J_c = 3.8$ kA/cm². Tape (b) had two heat treatments and was pressed at 0.5 GPa; $H^* = 100 \pm 20$ mT, and $J_c = 9.6$ kA/cm². Tape (c) had three heat treatments and was pressed at 2.0 GPa; $H^* = 230 \pm 20$ mT and $J_c = 14.5$ kA/cm².

of the sheath for electric fields between 1 and 100 μ V/cm, all subsequent analysis was done on the characteristics taken after the Ag had been removed.

Figure 4 shows $E(J)$ characteristics of the three heat treatment 2 GPa tape over the four decades of electric field that are free from the effects of thermoelectric noise and general flux flow. The data were taken as a function of magnetic field applied orthogonal to the rolling plane of the tape, i.e., parallel to the nominal c axis. The curvature of all the characteristics changes from negative to positive with increasing applied field. Two widely used theories of dissipation in single crystal superconductors, the vortex glass¹⁷ and the collective flux creep models,¹⁸ both predict an $E(J)$ relation of the form:

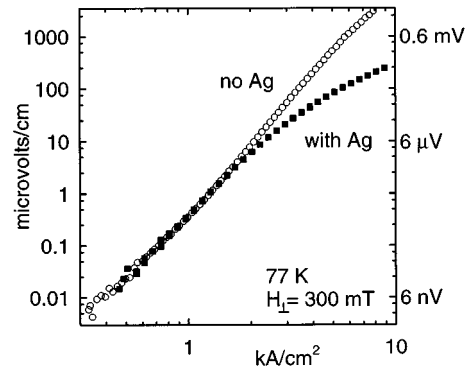


FIG. 3. This figure compares $E(J)$ characteristics of the 2.0 GPa, three heat treatment tape taken with and without its Ag sheath. Measured voltages appear on the right axis.

$$E = \rho J \exp[-(J_0/J)^\mu], \quad (1)$$

where $\mu > 0$, which has curvature in log-log space

$$\frac{\partial^2(\log E)}{\partial(\log J)^2} = -\mu^2(\log e) \left(\frac{J_0}{J}\right)^\mu$$

that is always negative. The exponential factor results in zero resistance for vanishing J ,

$$\frac{\partial E}{\partial J} = [1 + \mu(J_0/J)^\mu] \rho \exp[-(J_0/J)^\mu] \xrightarrow{J \rightarrow 0} 0.$$

This limit of nondissipative current flow means that Eq. (1) can only describe $E(J)$ below the irreversibility line. The negative curvature of data at lower fields in Fig. 4 is thus consistent with theories of irreversible behavior, while the positive curvature of data at higher applied field is not, to the extent that the shape of measured characteristics extends to arbitrarily low E . Following convention,^{4,5,19} we define the field at which the curvature of $E(J)$ changes sign as the irreversibility field $H^*(77$ K). According to the vortex glass and collective flux creep models, this criterion defines the boundary between reversible and irreversible behavior. It

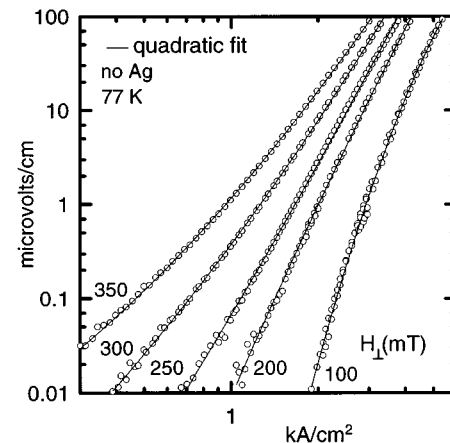


FIG. 4. The graph shows $E(J)$ characteristics for the bare tape of Fig. 2(c) at five applied magnetic fields. The quadratic fit measures the curvature of each characteristic in log-log space. The field at which the curvature changes sign for this tape is $H^* = 230 \pm 20$ mT.

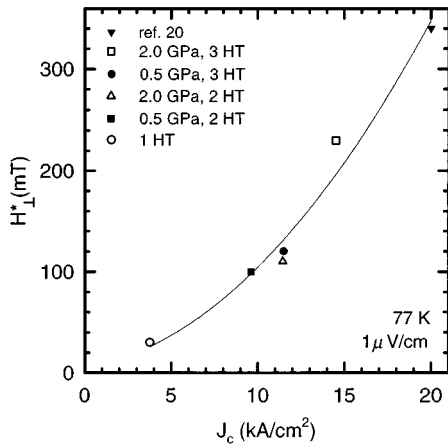


FIG. 5. H^* as measured in Fig. 4 is plotted vs J_c for all tapes in this study and one Bi-2223 tape from Ref. 19. The line is a guide to illustrate the correlation.

constitutes a transport method of measuring H^* that probes only those parts of the sample which lie in the current path, whereas H^* based on a measurement of magnetic moment may be sensitive to closed loops that circulate on smaller length scales than the voltage tap separation of the transport current measurement.

Figure 5 reveals a close correlation between increasing H^* and increasing $J_c = I_c/A$. One datum corresponds to each of the five tapes in the study. H^* rises steeply from 30 mT after 1 heat treatment to 230 mT after 3 heat treatments. Moreover, increased deformation pressure raised H^* too, for example from 120 to 230 mT at the third heat treatment. Corresponding to these changes in H^* , J_c increased from 3.8 to 14.5 kA/cm². The steepening slope of the correlation with increasing J_c suggested a test at higher J_c values. To demonstrate that the correlation continues to higher J_c , the plot includes the result of a similar transport extended $E(J)$ experiment from Li *et al.*¹⁹ for a tape with $J_c = 20$ kA/cm². Apart from this correlation, two trends are apparent from the plot. Tapes pressed at 2 GPa have larger H^* and J_c than those pressed at 0.5 GPa, and for either deformation pressure, both H^* and J_c increase with each heat treatment. Figure 6 illustrates the evolution in applied field dependence of J_c with heat treatment and pressing at 2 GPa. As the tape is processed further, J_c increases and its field dependence also grows weaker. The effect is even more marked in the field dependent J_c than in the zero field J_c . Tapes pressed at 0.5 GPa also showed this effect. This result indicates that H^* also correlates to J_c in a field.

IV. DISCUSSION

We frame our discussion of the changes in $J_c = I_c/A$ as a function of processing by recalling that this common definition of J_c is a macroscopic one, in which the measured transport critical current is normalized by the total cross-sectional area of all the phases making up the BSCCO core. Thus it is not enough to only consider changes in the easily measured I_c as a function of a process variable. To understand what is happening at a fundamental level, it is also desirable to un-

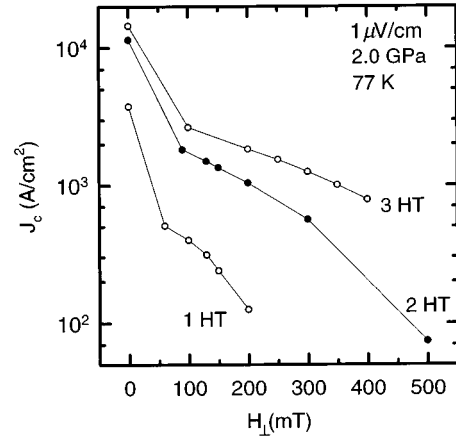


FIG. 6. J_c is plotted vs applied field for the 2.0 GPa tapes after each of three heat treatments. As J_c increases with continued processing it also becomes less field sensitive.

derstand how the active cross-section is changing. This is a very challenging task, so far only accessible by experiments such as microslice^{6,20} or MO imaging,⁷⁻⁹ in which the local J_c is probed on scales much smaller than the transport measurement. Unfortunately, it was not feasible to perform these experiments on these samples, although an extensive MO imaging experiment has been performed on a sample of the three heat treatment, two GPa tape.⁷

One important factor underlying the improvement in J_c with heat treatment concerns the phase changes that are occurring in the tape during heat treatment. Conversion of the starting 2212, CuO, and AEC phases to 2223 during thermo-mechanical processing increases the superconducting fraction of the core. One contribution to the rise in J_c with heat treatment should thus be roughly in proportion to the increase in superconducting fraction. Figure 2 shows that the first heat treatment sample is about half 2223 and has a J_c of 3.8 kA/cm². The third heat treatment sample in Fig. 2 has approximately twice as much 2223 but about four times the J_c (14.5 kA/cm²). Thus, the growth in 2223 volume fraction can account for only part of the increase in J_c . However, in addition to increasing the 2223 volume fraction, the thermo-mechanical processing also increases the density of the 2223 core,¹ and may also improve the grain alignment. The marked enhancement of the irreversibility field indicates that thermomechanical processing also improves the local properties of the superconductor, apparently by producing stronger flux pinning. The correlation between J_c and H^* illustrated in Fig. 5 implies that the increase in J_c is associated at least partly with increases in the flux pinning capability of the 2223 phase, and does not result exclusively from the increase in 2223 phase fraction. The simplest interpretation of such a correlation over a broad range of heat treatments and deformation pressures, is that of a flux pinning limited J_c .

The ability of Eq. (1) to describe $E(J)$ in CuO₂-based superconductors has been established in studies on single crystals of several materials.^{18,21} Li *et al.* demonstrated that it also describes $E(J)$ in polycrystalline 2223 tapes over a wide range of E and T .^{19,22} This led them to conclude that vortex

motion *within* 2223 grains is the source of the measured electric field and that intragranular flux pinning is the current-limiting mechanism.⁵ However, dissipation in the tapes may be more complicated than this. Wang *et al.*¹⁰ have directly compared the $E(J)$ characteristics within one grain to those across the grain boundary of an 8° [001] tilt $\text{Bi}_2\text{Sr}_2\text{CaCu}_2\text{O}_x$ (2212) bicrystal. Both sets of $E(J)$ curves show the change of curvature with applied field typical of the characteristics published by Li *et al.*^{5,19} and of those in Fig. 4. However, the *values* of J_c and H^* across the boundary were depressed by about 30% relative to those within a grain (a qualitatively similar result has since been obtained on several bicrystals¹¹). This result shows that low angle grain boundaries can provide an additional limit on the J_c properties of the grain interiors and also supports the railway switch model of current transport. However we note that nothing in the polycrystalline experiments defines the active area through which the current actually flows. In this case, our conclusion that the *critical current* is limited by flux pinning says nothing definite about the magnitude of the local *critical current density*. This is less true of the bicrystal experiment in that the dimensions of the bicrystal were well defined by laser cutting. However, intercomparison of 2212 and 2223 J_c values is uncertain. Thus we take from the 2212 bicrystal experiments only the conclusion that this is certainly a system in which the current-limiting mechanism appears to be the same in both grain and grain boundary *but* that it is also one for which the magnitude of J_c across the grain boundary is measurably less than within the grain.

The analogy between these tapes and the bicrystal extends to their field dependent behavior (Fig. 6). Although the bicrystal J_c showed a stronger field dependence across the boundary than within a grain, there was no evidence of Josephson behavior in the boundary characteristics. Figure 6 shows that tapes pressed at 2 GPa had the same inverse correlation between the magnitude of J_c and its field dependence. Thus, we consider a conclusion that J_c is only limited by the strength of intragranular flux pinning^{4,5} to be incomplete. We note two qualifications. The first is that dissipation by flux motion can occur anywhere in the current path, including grain boundaries, and is not confined to the interior of grains. The second is that any barriers to current flow, whether cracks, resistive grain boundaries, or low angle grain boundaries with slightly reduced H^* , can significantly affect J_c , as defined by I_c/A , through the influence that they have on confining the long range transport current I_c to only a fraction of the total cross-section A . As specific evidence for this point we cite the MO imaging by Pashitski *et al.*⁹ of 2223 tapes essentially identical to those used in this study, which showed an irregular, percolative current path that changed dramatically with both magnetic and electric field.

An important detail of the manner in which thermomechanical processing can improve flux pinning at 77 K is through conversion of residual 2212 intergrowths at some 2223 grain boundaries into 2223 phase. Energy dispersive x-ray (EDX) and XRD analysis of cross-sections like those in Fig. 1 indicated that the majority of this conversion occurs early in the process, predominantly during the first and second heat treatments. Nonetheless, Umezawa *et al.*³ observed

2212 intergrowths at (001) twist boundaries by transmission electron microscopy (TEM) in one-powder tapes whose 2212 content was not detectable by the x-ray or SEM techniques. Such intergrowths can significantly limit J_c because the 2212 layers must be proximity coupled to their 2223 phase “banks” for them to transport supercurrent. The destruction of this proximity coupling by increasing field generates an extra step in the magnetic susceptibility versus temperature trace.³ However, this step was absent from the traces of the tapes used in this study. Thus, we conclude that residual 2212 intergrowths alone cannot account for the processing-induced increase in J_c and H^* observed in the present two-powder tapes.

The deformation portion of the thermomechanical processing is intended to increase the grain alignment and the 2223 core density.¹ The sequence of SEM images shown in Fig. 2 suggests that both processes occur, coinciding with the rise in H^* (which indicates enhanced flux pinning within the current path). We suppose, although we could not explicitly verify, that the alignment of the grains within the current path improves during the processing. If our interpretation of the 2212 bicrystal studies is correct, then we would expect that flux pinning (and H^*) in a strongly coupled (non-Josephson) grain boundary would improve as the misorientation angle decreases. Thus, one interpretation of the enhanced H^* observed in the tapes is that the average misorientation angle is reduced by thermomechanical processing. Additional heat treatments form new connections between grains that can provide shunts around high angle boundaries in the current path. The real complexity of the optimization of 2223 tapes is that the same deformation treatment that better aligns the grains also forms cracks between the grains. Thus, for too great a number of deformation treatments, it is possible to envisage a situation where H^* continues to increase because flux pinning and grain alignment is improved, while at the same time the connected cross-section declines due to the formation of cracks during the deformation step which cannot be healed in the subsequent heat treatment. Aspects of this problem have been addressed by Parrell *et al.*^{23–25}

V. SUMMARY

Extended $E(J)$ characteristics of bare 2223 cores as a function of the number of heat treatments and deformation pressure provided a measurement of J_c and H^* sensitive to only those parts of the tape lying in the supercurrent path. We found that J_c and H^* were improved by increasing the deformation pressure and the number of heat treatments. We showed that multiple factors contribute to determining J_c , where J_c is defined by the quotient I_c/A . One factor is the increase in phase purity of the tape as heat treatment proceeds, while a second is the increase in flux pinning associated with the rise in H^* . Some of this rise is due to changes in the phase purity of the individual grains, and part to the properties of the grain boundaries. Thus the mechanisms that limit J_c are both microscopic, occurring at the nanoscale of both the grain and the grain boundary, and macroscopic on the scale of the second phase and crack size.

ACKNOWLEDGMENTS

We are very grateful to S. E. Dorris (Argonne National Laboratory) for the supply of the two component BSCCO powder. This work was supported by ARPA (N00014-90 J-4115) and EPRI (RP8009-05).

- ¹J. A. Parrell, S. E. Dorris, and D. C. Larbalestier, *Physica C* **231**, 137 (1994); *Adv. Cryo. Eng.* **40**, 193 (1994).
- ²B. Hensel, J. C. Grivel, A. Jeremie, A. Perin, A. Pollini, and R. Flukiger, *Physica C* **205**, 329 (1993); B. Hensel, G. Grasso, and R. Flukiger, *Phys. Rev. B* **51**, 15 456 (1995).
- ³A. Umezawa, Y. Feng, H. S. Edelman, Y. E. High, D. C. Larbalestier, Y. S. Sung, and E. E. Hellstrom, *Physica C* **198**, 261 (1992); A. Umezawa, Y. Feng, H. S. Edelman, T. C. Willis, J. A. Parrell, D. C. Larbalestier, G. N. Riley, and W. L. Carter, *ibid.* **219**, 378 (1994).
- ⁴K. Shibusaki, Q. Li, R. L. Sabatini, and M. Suenaga, *Appl. Phys. Lett.* **63**, 3515 (1993).
- ⁵Q. Li, H. J. Wiesmann, and M. Suenaga, *Appl. Phys. Lett.* **66**, 637 (1995).
- ⁶D. C. Larbalestier, X. Y. Cai, Y. Feng, H. Edelman, A. Umezawa, G. N. Riley, and W. L. Carter, *Physica C* **221**, 299 (1994); G. Grasso, B. Hensel, A. Jeremie, and R. Flukiger, *ibid.* **241**, 45 (1995).
- ⁷A. E. Pashitski, A. Polyanskii, A. Gurevich, J. A. Parrell, and D. C. Larbalestier, *Physica C* **246**, 133 (1995).
- ⁸U. Welp, D. O. Gunter, G. W. Crabtree, J. S. Luo, V. A. Maroni, W. L. Carter, V. K. Vlasko-Vlasov, and V. I. Nikitenko, *Appl. Phys. Lett.* **66**, 1270 (1995).
- ⁹A. E. Pashitski, A. Polyanskii, A. Gurevich, J. A. Parrell, and D. C. Larbalestier, *Appl. Phys. Lett.* **67**, 2720 (1995).
- ¹⁰J. L. Wang, I. F. Tsu, X. Y. Cai, R. J. Kelley, M. D. Vaudin, S. E. Babcock, and D. C. Larbalestier, *J. Mater. Res.* **11**, 868 (1996).
- ¹¹J.-L. Wang, Ph.D. thesis, University of Wisconsin-Madison, 1996.
- ¹²J. H. Cho, M. P. Maley, J. O. Willis, J. Y. Coulter, L. N. Bulaevskii, P. Haldar, and L. R. Motowidlo, *Appl. Phys. Lett.* **64**, 3030 (1994).
- ¹³Y. Hakuraku and Z. Mori, *J. Appl. Phys.* **73**, 309 (1993).
- ¹⁴H. Yamasaki, K. Endo, S. Kosaka, M. Umeda, S. Yoshida, and K. Kajimura, *Phys. Rev. Lett.* **70**, 3331 (1994); *Phys. Rev. B* **50**, 12 959 (1994).
- ¹⁵P. Wagner, U. Frey, F. Hillmer, and H. Adrian, *Phys. Rev. B* **51**, 1206 (1995).
- ¹⁶S. E. Dorris, B. C. Prorok, M. T. Lanagan, S. Sinha, and R. B. Poeppel, *Physica C* **212**, 66 (1993).
- ¹⁷M. P. A. Fisher, *Phys. Rev. Lett.* **62**, 1415 (1989); D. S. Fisher, M. P. A. Fisher, and D. A. Huse, *Phys. Rev. B* **43**, 130 (1991).
- ¹⁸G. Blatter, M. V. Feigel'man, V. B. Geshkenbein, A. I. Larkin, and V. M. Vinokur, *Rev. Mod. Phys.* **66**, 1149 (1994).
- ¹⁹Q. Li, H. J. Wiesmann, M. Suenaga, L. Motowidlo, and P. Haldar, *Phys. Rev. B* **51**, 701 (1995).
- ²⁰M. Lelovic, P. Krishnaraj, N. G. Eror, and U. Balachandran, *Physica C* **242**, 246 (1995).
- ²¹R. H. Koch, V. Foglietti, W. J. Gallagher, G. Koren, A. Gupta, and M. P. A. Fisher, *Phys. Rev. Lett.* **63**, 1511 (1989).
- ²²Q. Li, H. J. Wiesmann, M. Suenaga, L. Motowidlo, and P. Haldar, *Phys. Rev. B* **50**, 4256 (1994).
- ²³J. A. Parrell, D. C. Larbalestier, and S. E. Dorris, *IEEE Trans. Appl. Supercond.* **5**, 1275 (1995).
- ²⁴J. A. Parrell, Y. Feng, S. E. Dorris, and D. C. Larbalestier, *J. Mater. Res.* **11**, 555 (1996).
- ²⁵J. A. Parrell, A. A. Polyanskii, A. E. Pashitski, and D. C. Larbalestier, *Supercond. Sci. Technol.* **9**, 393 (1996).